Science of the Total Environment 890 (2023) 164421

Contents lists available at ScienceDirect

Science of the Total Environment

journal homepage: www.elsevier.com/locate/scitotenv

# Large-scale nutrient and carbon dynamics along the river-estuary-ocean continuum

Norbert Kamjunke [a,*], Holger Brix [b], Götz Flöser [b], Ingeborg Bussmann [c], Claudia Schütze [d], Eric P. Achterberg [e], Uta Ködel [d], Philipp Fischer [c], Louise Rewrie [b], Tina Sanders [b], Dietrich Borchardt [f], Markus Weitere [a]

[a] Helmholtz Centre for Environmental Research - UFZ, Department of River Ecology, Brückstraße 3a, D-39114 Magdeburg, Germany
[b] Helmholtz-Zentrum hereon GmbH, Institute of Carbon Cycles, Max-Planck-Straße 1, 21502 Geesthacht, Germany
[c] Alfred-Wegener-Institut, Helmholtz Centre for Polar and Marine Research, Departments of Marine Geochemistry & Shelf Sea System Ecology, Am Handelshafen 12, 27570 Bremerhaven, Germany
[d] Helmholtz Centre for Environmental Research - UFZ, Department of Monitoring and Exploration Technologies, Permoserstr. 15, 04318 Leipzig, Germany
[e] GEOMAR, Helmholtz Centre for Ocean Research, Wischhofstr. 1-3, 24148 Kiel, Germany
[f] Helmholtz Centre for Environmental Research - UFZ, Department of Aquatic Ecosystem Analysis, Brückstraße 3a, D-39114 Magdeburg, Germany

## HIGHLIGHTS

- Nutrient and carbon fluxes are key processes in land-ocean interactions.
- We sampled along the river-estuary-ocean system according to travel time of water.
- The river was autotrophic with phytoplankton growth, high pH and oxygen concentration, and $CO_2$ undersaturation.
- Phytoplankton died off in the estuary causing low pH and oxygen concentration, $CO_2$ supersaturation, and nutrient release.
- The approach is suitable to investigate single events such as hydrological extremes.

## GRAPHICAL ABSTRACT

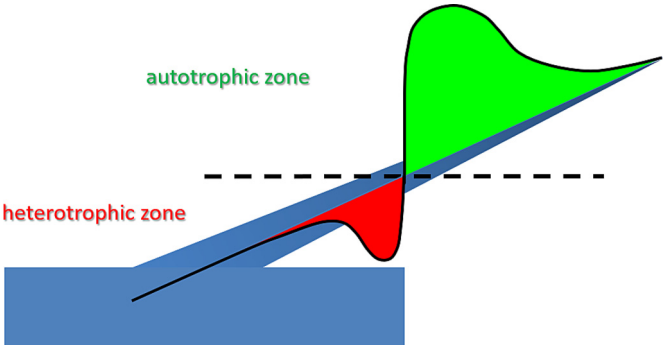


## ARTICLE INFO

Editor: Sergi Sabater

*Keywords:*
River-ocean continuum
Phytoplankton
Nutrients
Oxygen
pH
Autotrophic
Heterotrophic

## ABSTRACT

Nutrient and carbon dynamics within the river-estuary-coastal water systems are key processes in understanding the flux of matter from the terrestrial environment to the ocean. Here, we analysed those dynamics by following a sampling approach based on the travel time of water and an advanced calculation of nutrient fluxes in the tidal part. We started with a nearly Lagrangian sampling of the river (River Elbe, Germany; 580 km within 8 days). After a subsequent investigation of the estuary, we followed the plume of the river by raster sampling the German Bight (North Sea) using three ships simultaneously. In the river, we detected intensive longitudinal growth of phytoplankton connected with high oxygen saturation and pH values and an undersaturation of $CO_2$, whereas concentrations of dissolved nutrients declined. In the estuary, the Elbe shifted from an autotrophic to a heterotrophic system: Phytoplankton died off upstream of the salinity gradient, causing minima in oxygen saturation and pH, supersaturation of $CO_2$, and a release of nutrients. In the shelf region, phytoplankton and nutrient concentrations were low, oxygen was close to saturation, and pH was within a typical marine range. Over all sections, oxygen saturation was positively related to pH and negatively to $pCO_2$. Corresponding to the significant particulated nutrient flux via phytoplankton, flux rates of dissolved nutrients from river into estuary were low and determined by depleted concentrations. In contrast, fluxes from the estuary to the coastal waters were higher and the pattern was determined by tidal current. Overall, the approach is appropriate to better understand land-ocean fluxes, particularly to illuminate the importance of these fluxes under different seasonal and hydrological conditions, including flood and drought events.

* Corresponding author.
*E-mail address:* norbert.kamjunke@ufz.de (N. Kamjunke).

http://dx.doi.org/10.1016/j.scitotenv.2023.164421
Received 24 January 2023; Received in revised form 4 May 2023; Accepted 21 May 2023
Available online 25 May 2023

## 1. Introduction

Rivers drain terrestrial environments and transport considerable amounts of particulate and dissolved matter to the ocean. The matter experiences significant transformation processes within the river and the adjacent estuarine and coastal systems. This is particularly the case for dissolved nutrients and carbon, which experience complex biogeochemical transformation processes, including utilisation by autotrophic and heterotrophic microbes and subsequent recycling. A transition of trophic state (Dodds and Cole, 2007) was frequently observed: While many large rivers with high phytoplankton biomass were autotrophic (King et al., 2013; Kamjunke et al., 2021), there was a shift to heterotrophic conditions in estuaries (Gattuso et al., 1998; Amann et al., 2012) although this is not an exclusive pattern and some estuaries were autotrophic (Maher and Eyre, 2012). So estuaries alter the nutrients and carbon dynamics before entering the coastal shelf sea.

The longitudinal dynamics of carbon and nutrients as well as the quantity and quality of the transported material are highly dependent on hydrological conditions, particularly the dynamics of discharge. While transport dominates at high discharge, transformations are more important at low discharge (pulse-shunt concept; Raymond et al., 2016). Discharge variability is likely to increase as hydrological extremes are projected to occur more frequently in future (Hari et al., 2020). To estimate the effect of hydrological extremes on riverine matter transport and processing we need focussed investigations during such events, which cover the total spatial gradients from the river to the ocean. So far, many studies have investigated matter transformations in separate portions of the river-ocean continuum over different periods of time. However, combined approaches measuring simultaneously in rivers, estuaries and coastal shelf regions are rare.

Most studies investigating the river-ocean continuum focussed on the salinity gradient: they started at the freshwater endmember and sampled along the estuary to the river plume in the shelf region (Abril et al., 2002; Olli et al., 2023). Often they detected a decrease in phytoplankton biomass and a composition change from freshwater species (diatoms, green algae) to marine phytoplankton (chrysophytes), e.g. in the Mackenzie River and the coastal Beaufort Sea (Retamal et al., 2008), in the Ob River estuary (Sukhanova et al., 2010), and from lower Yenisei River to the Kara Sea in Russia (Bessudova et al., 2014). However, these studies did not investigate the processes in the river itself—that is, longitudinal dynamics of carbon and nutrients over longer distances in the freshwater portion. To study the river, estuary and coastal water system in a holistic manner, the use of different ships is required, particularly under conditions of low discharge when small ships with low draught are needed in the upstream river, whereas seaworthy vessels sample the regions offshore. Furthermore, most of the previous studies sampled a number of discrete sites along the reach but did not measure continuously with probes. Here, we sampled a full gradient of freshwater river, estuary and coastal waters using different ships and continuous sensor records.

Understanding river-sea systems requires a thorough understanding of processes that span different Earth system compartments. Event-based multi-ship samplings were established within the MOSES initiative (Modular Observation Solutions for Earth Systems) instituted by the Helmholtz Association (Weber et al., 2022). The campaign involved four research vessels and spanned nearly two months. Measurements included standard hydrological and oceanographic parameters, as well as quantities relevant to the nutrient and carbonate system. We combined a Lagrangian approach used in river studies with subsequent measurements in the river-estuary-shelf system. The goal of the present study is a thorough understanding of the flux of carbon and nutrients from the land to the ocean, including the complex biogeochemical transformation processes within the water. For that, we analysed the different carbon and nutrient species and proxies for the biological transformation processes in a complex Langrangian approach from the river to the ocean. We quantified the growth of phytoplankton and intensive autotrophic processes in freshwater. Subsequently, we investigated the fate of the phytoplankton biomass and its heterotrophic consequences in the estuary and coastal waters. Although the estimation of nutrient fluxes in a tidal-affected system is difficult, we established an approach for the calculation of nutrient export to coastal waters. A holistic approach of nutrient budgets and transport to cover the entire river system has, to our knowledge, not yet been attempted.

## 2. Material and methods

### 2.1. Study area and sampling

General approach: Investigations were performed in the River Elbe in central and northern Europe, which is 1094 km long and drains a catchment of 148,268 $km^2$. In the river, a water "parcel" was investigated on the way downstream according to its travel time in order to follow the development of water quality which is dependent on allochthonous inputs by tributaries and on autochthonous processes, such as phytoplankton growth or degradation. In the freshwater section of the Elbe River, measurements were undertaken while moving with the water mass. In the estuary, the estimated average residence time of water at mean discharge was four weeks (Boehlich and Strotmann, 2008; Voynova et al., 2017), but matter fluxes were dominated by the twice daily alternating water mass transport up and down the estuary by the diurnal tides. Here, a sampling exercise of the same water body is not realistic, nor practically feasible. Instead, we sampled the estuary against the ebb current two weeks after the river portion, as in previous studies (Dähnke et al., 2008; Sanders et al., 2018). In the North Sea, the cruise covered a grid from the Weser and Elbe estuaries and along the west coast of Schleswig-Holstein up to the island of Sylt, as the river plumes spread along this coastline. Therefore, we coordinated three ships equipped with mostly identical sensor arrays to closely cover the target area. When combined with auxiliary tide gauge and throughflow data, the concentrations can be used to estimate along-river transport of water constituents. We developed this concept to investigate transport in various sections of the river and the estuary, and we estimated sources and sinks along the sections. Multi-ship sampling procedures were deployed, common strategies for data analysis across multiple domains were provided, and reference data for the main environmental parameters were created (e.g., Fischer et al., 2021; Bussmann et al., 2021; Bussmann et al., 2022).

#### 2.1.1. Freshwater river cruise, 4–12 Aug. 2020

We applied a Lagrangian approach using the RV *Albis*, whereby the ship was cruising eight hours with three-fold flow velocity of the river followed by a 16 h break every day (Kamjunke et al., 2022). We sampled the middle portion of the River Elbe, between Schmilka near the Czech-German border (km 4 according to German river kilometrage) and the Geesthacht Weir near Hamburg, upstream of the tidal zone which is free-flowing and undamed along a stretch of 585 km (Fig. 1). The cruise was performed in the period between 4 and 12 Aug 2020 at a low discharge (242 $m^3\ s^{-1}$ at Magdeburg). This corresponds approximately to the mean low discharge in summer (231 $m^3\ s^{-1}$ at Magdeburg). Samples were taken with a horizontal sampler from a water depth of 30 cm in the middle of the river.

#### 2.1.2. Tidal Elbe cruise, 25–26 Aug. 2020

The water flow in the tidal Elbe is subject to a different variability than in the fresh water section, and hence the time it takes a water parcel to travel between the weir in Geesthacht and the mouth of the estuary in Cuxhaven is between two and twelve weeks (Voynova et al., 2017). To capture approximately the same water mass, the tidal Elbe cruise (RV *Ludwig Prandtl* from Hereon) was conducted subsequently, approximately two weeks after the *Albis* cruise, which was half of the residence time of four weeks at mean discharge (Voynova et al., 2017). The cruise started from Cuxhaven on the 25th of August towards the island of Scharhörn. From there, the ship headed back to Glückstadt where it anchored from 15:00 to 06:00 h in order to cover a full tidal cycle. From Glückstadt, the ship continued upstream to Oortkaten, upstream of the city of Hamburg, until 16:15 h. Thirty-three samples were taken from the moving ship between Scharhörn and Oortkaten, and twelve samples (every hour) at the anchor station at Glückstadt.

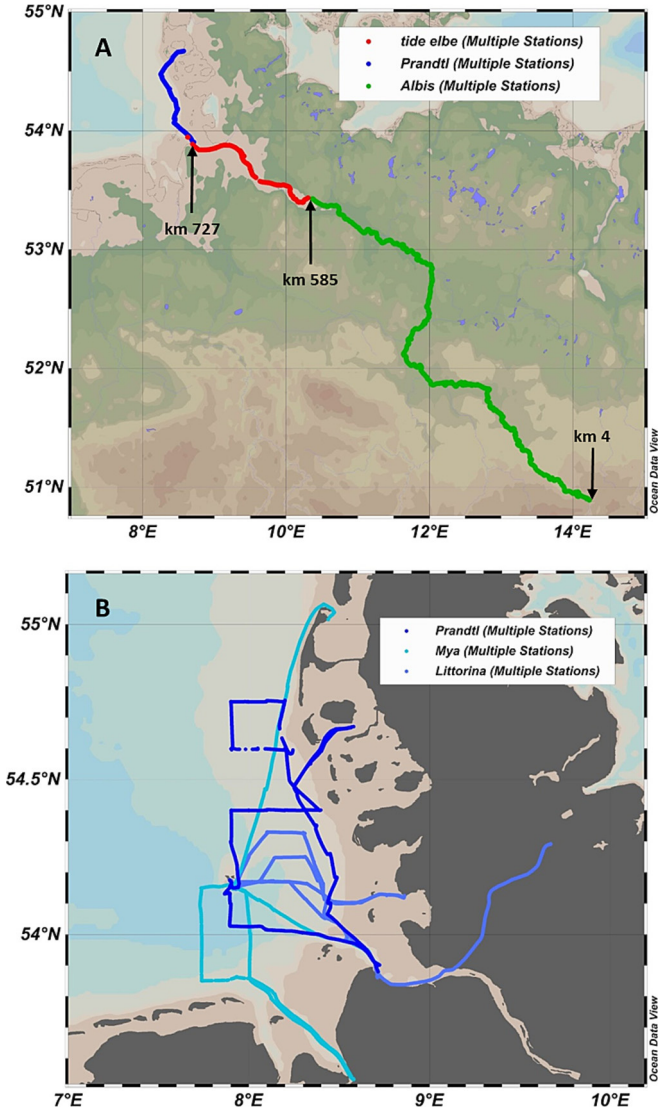


**Fig. 1.** A: Sampling stretches in the freshwater river (green), estuary (red) and coastal water (blue); B: detailed routes of three ships in coastal waters.

*2.1.3. German Bight cruise, 31 Aug. – 3 Sep. 2020*

With three research vessels (RV *Littorina* from GEOMAR, RV *Mya II* from AWI and RV *Ludwig Prandtl* from Hereon), a wide coastal area was covered over a period of 4 days, from 7.7°E to 8.7°E and from 53.4°N to 55.1°N (Fig. 1; Bussmann et al., 2021). Areas with higher salinity were observed around Helgoland and towards the west, while areas of reduced salinity (approximately 30) extended more towards the north. This indicates that the river plumes from Elbe and Weser mainly flow along the west coast of Schleswig-Holstein. The circulation calender (https://www.bsh.de/DE/DATEN/Vorhersagen/Stroemungen/Zirkulationskalender/zirkulationskalender_node.html) confirmed a cyclonic, counter-clockwise current direction in the North Sea on Sep 3rd so that the Elbe River water was directed northwards. The temperature distribution was rather uniform, with unexpected warm water north of the Frisian islands and east of Amrum. The water column was well mixed at all stations and no stratification or difference between surface and bottom water was observed. For the entire longitudinal analysis, river kilometrage was used (https://atlas.wsv.bund.de/bwastr-locator/client/) and continued for the tidal Elbe and North Sea portion, following the course of the RV *Ludwig Prandtl* on the 3rd of September.

*2.2. Laboratory analyses*

Standard methods were applied for chemical sample preparations and analysis as described previously (Kamjunke et al., 2013), including use of all German standards. Nitrite ($NO_2^-$), nitrate ($NO_3^-$), and silicate (Si) were spectrophotometrically determined using a segmented flow technique; total phosphorus (TP) and phosphate were measured using the ammonium molybdate spectrophotometric method. For chlorophyll *a* analysis, samples were filtered onto glass fibre filters (GF-F, Whatman, Buckinghamshire, UK) immediately after sampling, filters were frozen, and chlorophyll *a* was measured using high performance liquid chromatography after ethanol (Kamjunke et al., 2021) or acetone extraction (Zapata et al., 2000).

Inorganic (IC), organic (OC) and total (TC) carbon concentrations in filtered and unfiltered water samples were analysed based on high temperature oxidation using NDIR-detection. For POC (particulate organic carbon) determination, 500 ml of water was filtered on pre-combusted GF-F filters (nominal pore size 0.7 μm) and stored frozen (−20°). For DOC, water was filtered and preserved with ultraclean HCl. In the home laboratory, filters and DOC were analysed with a DIMATOC 2000 (Dimatec Analysentechnik GmbH, Essen, Germany) or an elemental analyzer, Eurovector. For marine DIC (dissolved inorganic carbon) samples, 20 ml glass vials were filled with sample water and preserved with $HgCl_2$. In the home laboratory the samples were analysed using a DIC analyzer (Apollo Scientific). All sampling and analysis procedures followed standard protocols (Dickson et al., 2007).

Basic hydrographic parameters (temperature, salinity, conductivity, oxygen, turbidity and chlorophyll) were measured with ferrybox systems mounted on the research vessels *Mya II* and *Ludwig Prandtl*, and with portable ferryboxes on the *Albis* and *Littorina* (Petersen, 2014).

Green house gas (GHG) concentrations in ambient air were measured with the LI-7810 $CH_4/CO_2/N_2O$ Trace Gas Analyzer (LI-COR Biosciences, Lincoln, NE, United States), which is a laser-based gas analyzer that uses optical feedback cavity-enhanced absorption spectroscopy. The analyzer was installed on the top deck of the *Albis* and afterwards on the *Ludwig Prandtl*, and measurements were obtained continuously at a sampling frequency of 1 Hz. Due to the internal flow rate and use of a 2 m tube, there was a small delay of 1 s between the tube inlet and the detector. The analyzer provided the dry mole fractions of $CO_2$ [ppm] (and $CH_4$) corrected for air for both spectroscopic interference and dilution due to water vapour. Unpublished tests of the device setup under ambient air conditions showed a precision of 1.5 % for $CO_2$ measurements. All sampled data were averaged over 1 min and quality-checked, resulting in a range of 383–455 ppm, and merged with the position data.

*2.3. Calculations*

For the conversion of conductivity to salinity, the R Package gsw (1.0–6) was used, and for the calculation of the water density, R Package oce (1.7–8) was used. To calculate $pCO_2$ based on pH and DIC, we used the R package seacarb (3.3.1, carb, flag9) with the respective values for temperature, salinity and silicate concentration. The partial pressure of $CO_2$ ($pCO_2$) was determined with the unit "μatm" or as "ppm" ($p2xCO_2$). The difference between the partial pressure of $CO_2$ in water and the measured atmospheric concentration (both in ppm), was termed delta. Positive values indicate an oversaturation of $CO_2$, whereas negative values indicate an undersaturation of $CO_2$.

*2.4. Determination of fluxes and mass transport*

In general, the mass transport reported here was calculated by multiplying discharge values with measured concentrations of water column constituents. Discharge of the freshwater Elbe River was calculated using the hydrodynamic model Hydrax (Oppermann et al., 2015). For the tidal portion of the Elbe, discharge was calculated using the Semi-implicit Cross-scale Hydroscience Integrated System Model (SCHISM; Zhang et al., 2016). SCHISM solves the Reynold-averaged Navier-Stokes equations in

three spatial dimensions on unstructured meshes (Zhang et al., 2016). The model has been set up for the area of the German Bight, including the Elbe Estuary, coupling it to the forcing from operational ocean and atmospheric reanalyses (Stanev et al., 2019). The simulations account for sea level variations, currents and thermohaline dynamics on tidal to annual time scales which are solved on horizontal spatial scales ranging from 1 km in the outer German Bight to 30 m in the Elbe Estuary. River discharge data used as a forcing at the tidal weir has daily time resolution. The estuarine water fluxes are a function of river discharge, tides, wind and baroclinic processes. During model integration, the volume fluxes across given cross-transects have been calculated and written out at every model time step of 100 s.

For the tidal portion of the Elbe River, there is a need to account for the influence of tidal variability when determining the net mass transport. Ideally, this would be done using long-term records at numerous positions along the river. Unfortunately, the only permanent water constituent measurements available are from the Cuxhaven FerryBox station (Elbe km 727; Baschek et al., 2017). In addition, our measurements in the tidal Elbe include a full tidal cycle with hourly values measured at an anchored station off Glückstadt (Elbe km 673.35). These measurements can be used to correct the in-situ values, accounting for the phase of the tidal cycle. This was done by determining for each measurement the time Δt after low tide at its respective location and time of measurement. For the time series at Glückstadt and Cuxhaven, we determined for each quantity the deviation of the respective values from their mean value at time Δt. The deviations of the values from their mean at Glückstadt were sufficiently small (between 10 and 20 % for phosphate, nitrate, silicate and ammonium, and approximately 30 % for nitrite) that we can account for this deviation as part of the general measurement uncertainty. For Cuxhaven, the deviations are larger (approximately 30 % for all quantities), but other sources of uncertainty (such as a lack of measurements to resolve the actual flow at any river cross-section) introduce larger errors in this calculation. As we neither have any direct information on the decline of deviations between Cuxhaven and Glückstadt and beyond, nor a reliable proxy, the use of mean values is preferable over interpolations and extrapolations that would just introduce additional error sources. In addition, for the purpose of this study, we target a mean matter transport. That is, using mean values for our calculations is a reasonable approach. The mean concentration values have then been multiplied with the average discharge model value of 250 $m^3\ s^{-1}$ (value at Neu-Darchau, km 536.4) under the assumption that the net contribution of freshwater sources and sinks and their variability along the tidal Elbe is negligible.

## 3. Results

Salinity measurements indicated low values in the upstream portion of the River Elbe until km 290 (Fig. 2). After the confluence with the River Saale, salinity increased sharply from <0.3 to 0.5 PSU and showed a higher variability due to the delayed lateral mixing of salt-rich waters from the tributary. Salinity further increased along the estuary towards the coast. The variability in the tidal section of the river was caused by the ebb and flow stream as recorded at the overnight station off Glückstadt, reflecting the inflow of salt-rich water and the outflow of less salty water. Salinity in the tidal Elbe ranged from 0.5 to 6.5. Salinity in the German Bight was nearly constant, ranging from 16.0 to 33.0 PSU, with a median of 30.3.

Water temperature was approximately 21 °C in the upper region and increased along the freshwater stretch, reaching a maximum of 26.8 °C with an overall median of 25.2 °C. Data showed typical diurnal dynamics with low values in the morning and higher values in late afternoon. Temperature was lower in the estuary, ranging from 20.7 °C to 23.1 °C with a median of 22.0 °C. In coastal waters, temperature ranged from 18.0 to 21.5 with a median of 19.2 °C.

Concentrations of chlorophyll *a* declined slightly in the upper reaches and increased to a maximum of 48.5 μg $L^{-1}$ at km 450 (Fig. 3). Values decreased in the slow-flowing downstream portion, likely due to sedimentation. Minimum chlorophyll concentrations (1.27 μg $L^{-1}$) were observed in the estuary (km 676). Values in the North Sea were relatively low and decreased from the coast towards the open North Sea. The concentrations of dissolved nutrients showed an inverse pattern to chlorophyll: silicate, nitrate and phosphate started from high values in the upstream third of the river stretch (110, 160 and 3.2 μmol $L^{-1}$, respectively), declined when phytoplankton started to grow, and were depleted to low values (50, 18 and 0.1 μmol $L^{-1}$, respectively) in the downstream river. In contrast, nutrient concentrations started to rise at the location of minimum of chlorophyll values and were highest just upstream of the salinity gradient maximum, before dropping again in the marine environment. Inorganic nitrogen was dominated by nitrate, whereas the concentrations of ammonium and nitrite were two and three orders of magnitude lower, respectively, and have distinct peaks in the Hamburg Port region. Additionally, there is a second peak in the salinity gradient. When concentrations of dissolved nutrients were plotted as a function of salinity (Fig. S2), a negative relationship was observed for phosphate, nitrate, nitrite, and silicate between 10 and 30 PSU, indicating dilution for the short distance between km 700 and km 730. In contrast, ammonium concentration increased.

Oxygen saturation was below 100 % (minimum of 72 %) in the upstream portion (Fig. 4). Coinciding with the presence of enhanced levels of phytoplankton biomass, oxygen saturation increased to maximum values of 190 % and showed a pronounced diurnal pattern with increasing saturation throughout the day. Oxygen saturation decreased in the downstream region of the river (to 75.8 %). The estuary was characterised by a distinct minimum in oxygen saturation in the region of Hamburg harbour at km 630 (40 %) and a subsequent increase further downstream. Saturation was approximately at equilibrium in the German Bight. Values of pH corresponded to oxygen saturation: an initial increase, maximum in the downstream region of the river, brackwater minimum, and higher values at sea. The plot of pH versus oxygen saturation indicates an overall positive relationship between these variables (Fig. 5). This was found not only within the individual river, estuary and coastal sections, but also across the compartments.

Carbon species are shown in aerial plots to include distributions in the German Bight (Figs. S5-S7). Dissolved inorganic carbon showed a wide range of lower values in the river (1644 to 2028 μmol $L^{-1}$, median 1808 μmol $L^{-1}$). In the tidal Elbe, DIC ranged from 1879 to 2164 μmol $L^{-1}$ (median 2021 μmol $L^{-1}$) and the highest values were observed in the marine area with 2038–2206 μmol $L^{-1}$ (median 2108 μmol $L^{-1}$). Dissolved organic carbon showed a low range of concentrations in the river (418–-783 μmol $L^{-1}$, median 564 μmol $L^{-1}$), while in the marine area a wider range of concentrations was covered (145–1996 μmol $L^{-1}$, median 319 μmol $L^{-1}$). Particulate organic carbon increased in the river from 95 μmol $L^{-1}$ at Schmilka towards 544 μmol $L^{-1}$ at km 506. Low values with a median of 512 μmol $L^{-1}$ were observed in the German Bight. Within the marine region, higher values were observed close to the shore and in estuaries.

The partial pressure $pCO_2$ ranged from 64 μatm at km 506 in the Elbe, to 2389 μatm at km 4 in the Elbe with a median of 603 μatm in the total river. Highest values were observed in the tidal Elbe, ranging from 1128 to 4710 μatm at km 644 with a median of 2285 μatm. In the marine area, $pCO_2$ ranged from 259 to 794 μatm with a median of 426 μatm. Atmospheric $CO_2$ concentrations along the River Elbe ranged from 383 ppm to 487 ppm with a median of 407 ppm. However, we also observed strong diurnal variations (Bussmann et al., 2022), which are not considered here. For the tidal Elbe and the marine area, atmospheric $CO_2$ was within a similar range and with a median of 404 and 401 ppm, respectively. The difference (delta) between $pCO_2$ in the water with the atmospheric $CO_2$ concentration reveals if the site was over- or undersaturated with $CO_2$ (Fig. 6). From km 54 to km 351 of the Elbe, the river was oversaturated with $CO_2$ with an average delta of 857 ± 600 ppm, followed by a region of undersaturated water (mean −281 ± 54 ppm), from km 388 to km 570. However, towards the weir in Geesthacht and in the subsequent tidal Elbe, maximal values of oversaturation were observed (average of 2209 ± 1323 ppm). The marine area, in contrast, was mostly near the equilibrium concentrations with an average of 30 ± 101 ppm. There was a strong negative logarithmic correlation

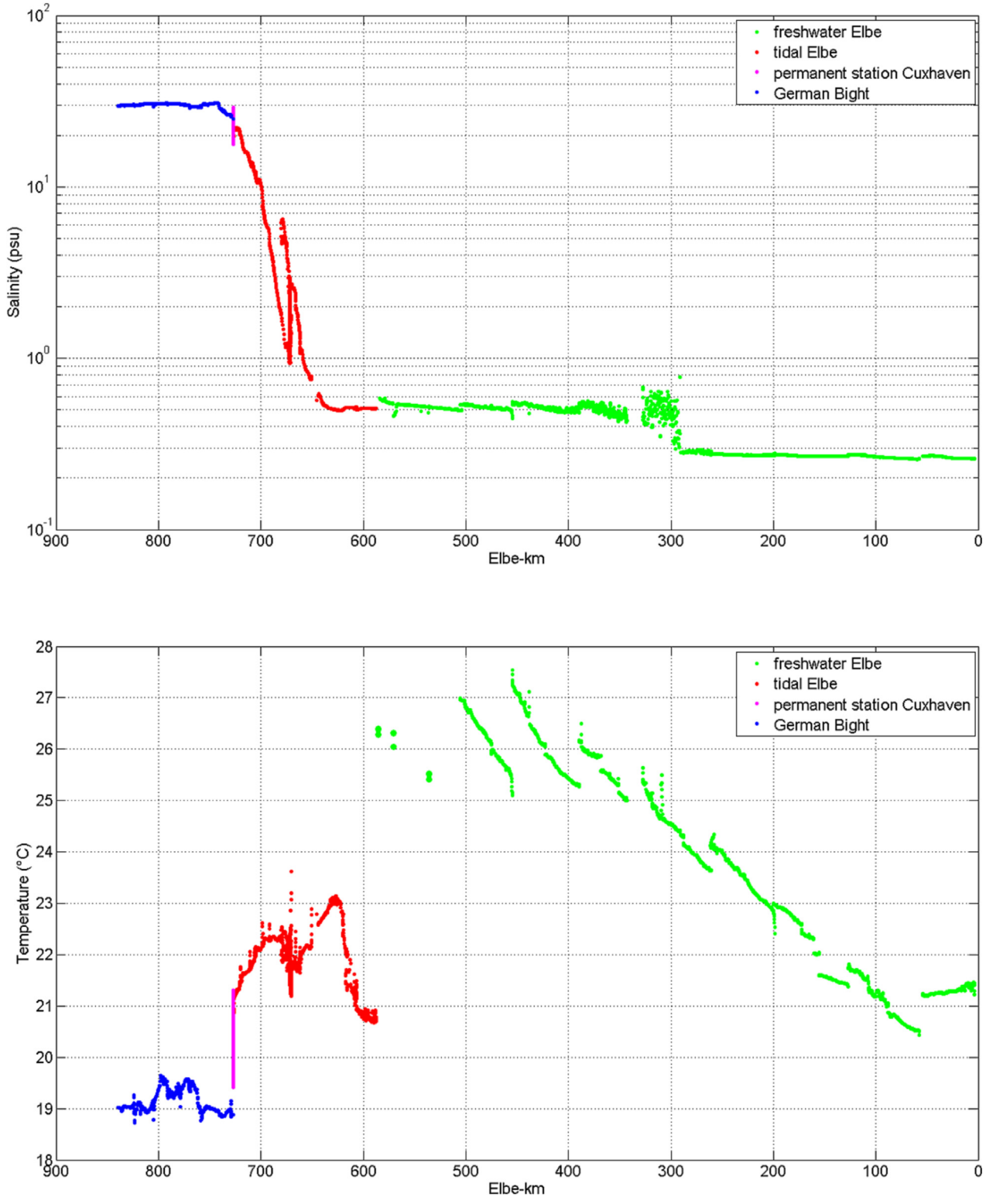


**Fig. 2.** Longitudinal dynamics of salinity and water temperature in the freshwater river (green), estuary (red) and coastal water (blue).

between $pCO_2$ and oxygen saturation ($r^2 = 0.91$) for the freshwater and estuary portion, while data from the marine area formed a distinct separate cluster (Fig. 7). The $pCO_2$ together with the oxygen saturation and pH values indicated the existence of an autotrophic zone in the river section with increasing autotrophy from upstream to downstream and a heterotrophic zone in the freshwater portion of the estuarine section. This is followed by a balanced situation in the marine sections.

Fluxes for dissolved phosphate, nitrate and silicate behaved similarly over the course of the river (Fig. 8): The fluxes were high in the upstream portions, with values decreasing towards the weir after uptake by phytoplankton. Downstream of the weir, their values increased steadily until approximately km 700, where the signal introduced by the tidal variations became too strong and the values decreased substantially. In contrast, nitrite and ammonium fluxes first decreased over the course of the freshwater

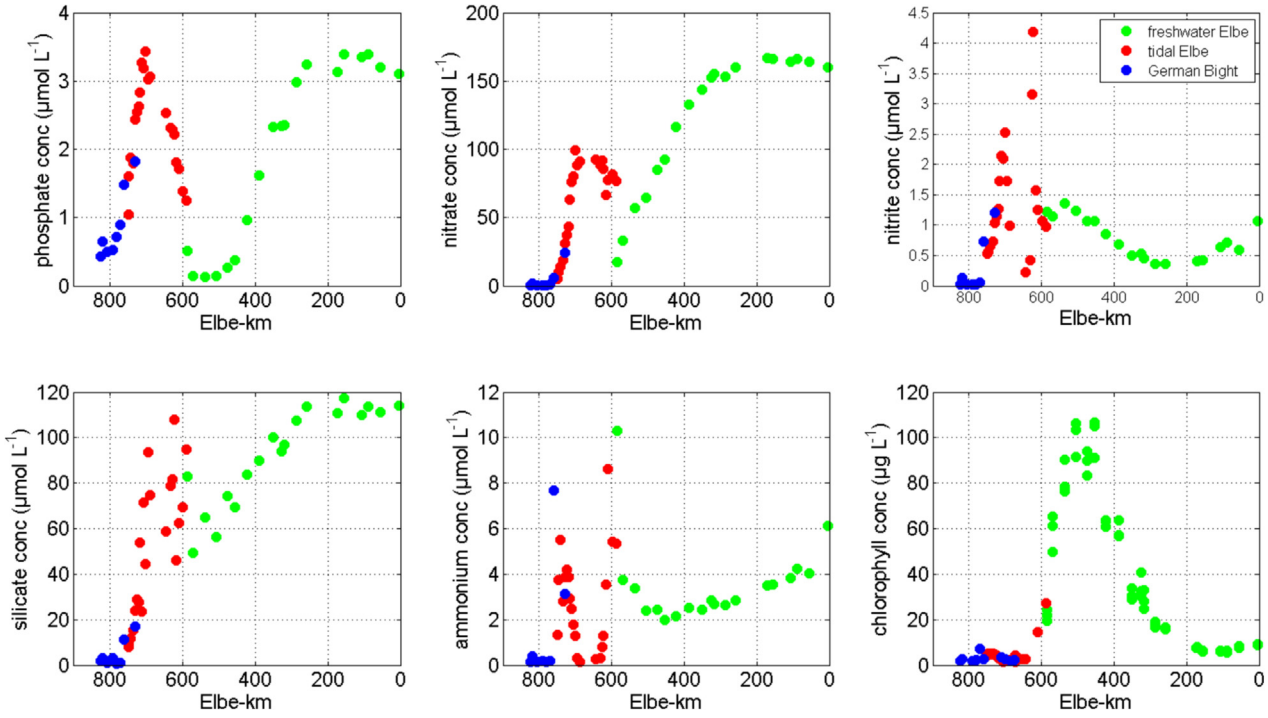


**Fig. 3.** Longitudinal dynamics of chlorophyll *a*, dissolved silicon, nitrate, nitrite, ammonium, phosphate along the River Elbe, estuary and coastal water.

portion of the river and then increased until the region of Hamburg Harbour (marked with HH in Fig. 8). There, the fluxes dropped precipitously and recovered further downstream. Past km 700, their trends diverged with a decrease in nitrite similar to those observed in phosphate, nitrate and silicate, while ammonium increased into the German Bight. This indicates input of organic matter from the marine portion into the estuarine portion. The two peaks of ammonium and nitrite indicate nitrification.

Tidal water movements had an influence on the Elbe downstream from the weir in Geesthacht. This influence increased towards the river mouth and was clearly discernable in the variations of the fluxes in Glückstadt and Cuxhaven (Fig. 9). Combining the tidal water flux with the concentrations of the nutrient species revealed a differentiated picture of the nutrient flux. For example, the nutrient flux variability was higher in Cuxhaven compared to Glückstadt for phosphate and nitrite, but smaller for nitrate and silicate (Fig. 9).

## 4. Discussion

Here we present a unique coordinated sampling campaign from upstream portions down to the estuary and coastal waters on a great number of proxies relevant to nutrient and carbon dynamics with respect to stocks and processes. The conditions match a low water period, thus allowing conclusions on the base-flow situation without significant surface runoff and allowing, to a certain extent, predictions of future situations under increasing droughts. The processes can be roughly categorized into three parts representing the major sections in the salinity gradient: the freshwater with increasing production along the river stretch, the estuary with high mineralization and release of inorganic nutrients, and the marine portion affected by the discharge of limiting nutrients from the land.

### *4.1. Increasing autotrophic production along the river continuum*

We observed a longitudinal increase of phytoplankton biomass under conditions of low discharge during our study period. During the first two observation days, phytoplankton biomass remained low at levels $<8\ \mu g\ L^{-1}$. In this section until river km 120, the Elbe River is free of groyne fields where phytoplankton may grow to higher densities and inoculate the main stem. Afterwards, chlorophyll concentration increased by a factor of ten up to 50 $\mu g\ L^{-1}$. The net growth observed in our study is typical for rivers with low grazing by benthic filter feeders (Ruiz Albizuri, 2018), which is the case in River Elbe (Hardenbicker et al., 2016). Maximum chlorophyll concentration detected in our study was lower than in former years at low discharge (90–180 $\mu g\ L^{-1}$; Kamjunke et al., 2021). High chlorophyll *a* concentrations are typically observed at low discharge only when light conditions are favourable (Turner et al., 2022). The growing phytoplankton biomass incorporated dissolved nutrients thereby shifting carbon and nutrients between the dissolved phase and particulate phase during production/degradation phases in the river-estuarine-continuum. Phosphate depletion was measured in the River Elbe before (Rode et al., 2007; Hardenbicker et al., 2016; Ritz and Fischer, 2019) and in other rivers (e.g., the River Thames; Bowes et al., 2012). Previous studies showed that seston C:P ratios in River Elbe increased and indicated phosphorus limitation as soon as phosphate was depleted (Kamjunke et al., 2021).

The Elbe River was autotrophic in the middle portion in summer (primary production: respiration ratio > 1; Kamjunke et al., 2021). The partial pressure of $CO_2$ ranged from 64 µatm in the middle region of the Elbe up to 2389 µatm. Such values have also been reported for other European rivers such as the Oder (1351 µatm; Stokowski et al., 2020). Previous studies for the Elbe estuary report approximately 400 µatm in summer (Voynova et al., 2019), or an undersaturation due to primary production with 141 µatm (Brasse et al., 2002). The concentration of dissolved $CO_2$ decreased, caused by increasing photosynthesis and the river was a $CO_2$ sink.

### *4.2. Heterotrophic breakdown and re-mineralization in the estuary*

Regarding the salinity gradient, most studies observed a decrease in phytoplankton biomass and dissolved nutrient concentrations from the downstream portion of the rivers towards the coastal waters, e.g., in the lower St. Johns River estuary in Florida (Wang and Zhang, 2020). The decline was often very pronounced and reached two orders of magnitude in the Segura River in Spain (Bazin et al., 2014). In the estuary of the Elbe River, we detected a minimum of phytoplankton biomass near km 620. Remarkably, the decline occurred upstream of the salinity gradient and was probably caused by sedimentation due to low flow

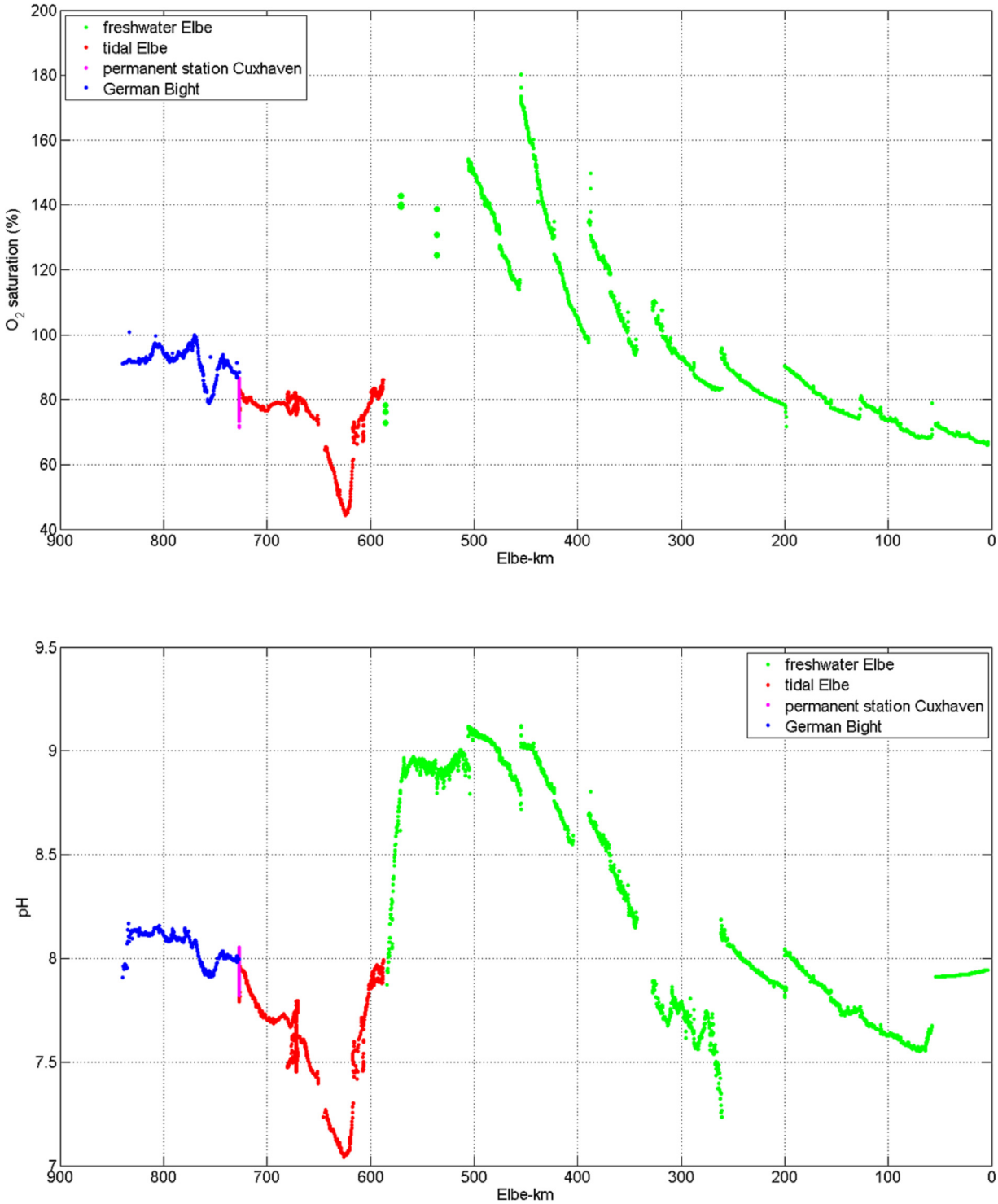


**Fig. 4.** Longitudinal dynamics of oxygen saturation and pH values in the freshwater river (green), estuary (red) and coastal water (blue).

velocity and the deeper water column, which reaches downward to 16 m in Hamburg Harbour. Simultaneous with phytoplankton decline, the river shows a well-known oxygen depletion immediately downstream from Hamburg Harbour that has been previously reported (Kerner, 2000; Amann et al., 2012; Schöl et al., 2014). Part of the oxygen depletion appears because of nitrification in the Elbe estuary (Sanders et al., 2018). In addition, phytoplankton degradation led to a release of all dissolved nutrients. This has been observed in other systems as well, where maximum concentrations of dissolved inorganic nitrogen and phosphorus and low values of dissolved oxygen were found in the estuary of Logan River in Australia (Saeck et al., 2013). There was also a simultaneous decline of phytoplankton and oxygen and an inverse pattern of nutrients reported for the lower St. Johns River estuary (Wang and Zhang, 2020). For the tidal part of the Elbe River as the transition zone from the riverine to the marine environment there is clear evidence that the concentrations and fluxes of nutrients are determined by the interplay of upstream transport into the system, anthropogenic influences from agricultural and industrial activities (nitrification, Hamburg Harbour), flow velocities and associated sedimentation rates, as well as tidal mixing processes.

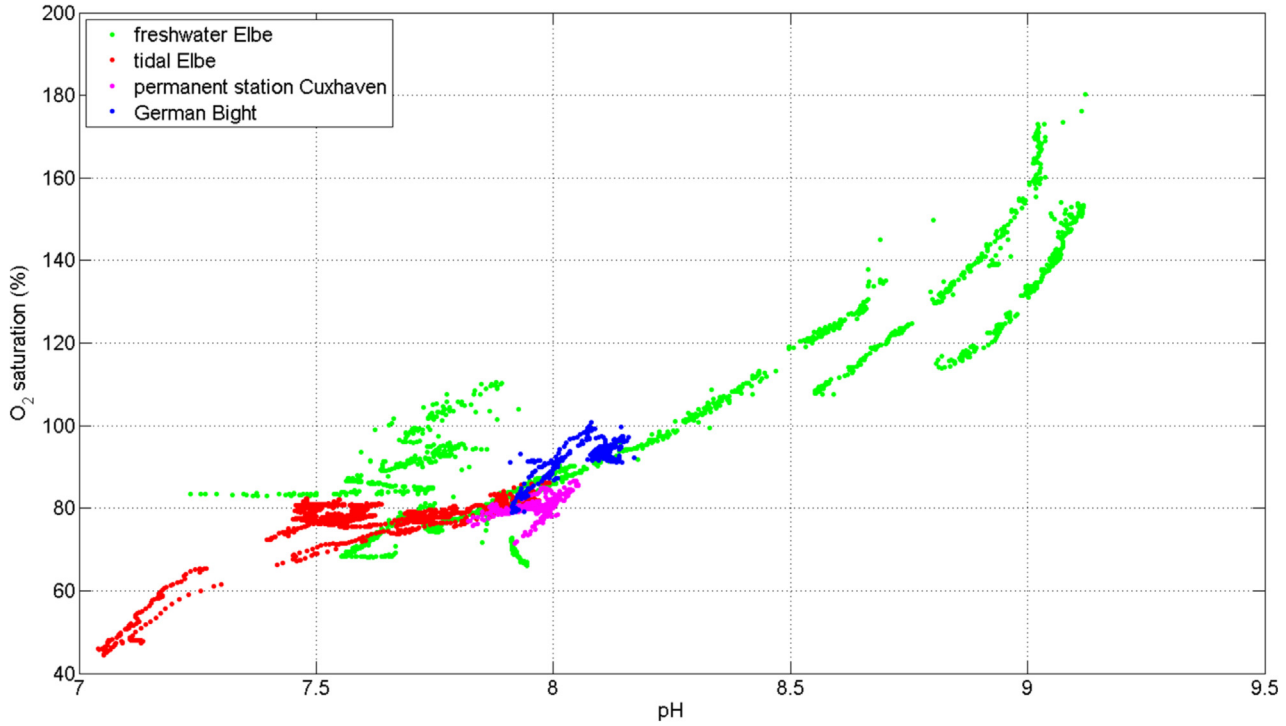


**Fig. 5.** Plot of oxygen saturation versus pH values of the River Elbe, estuary and coastal water.

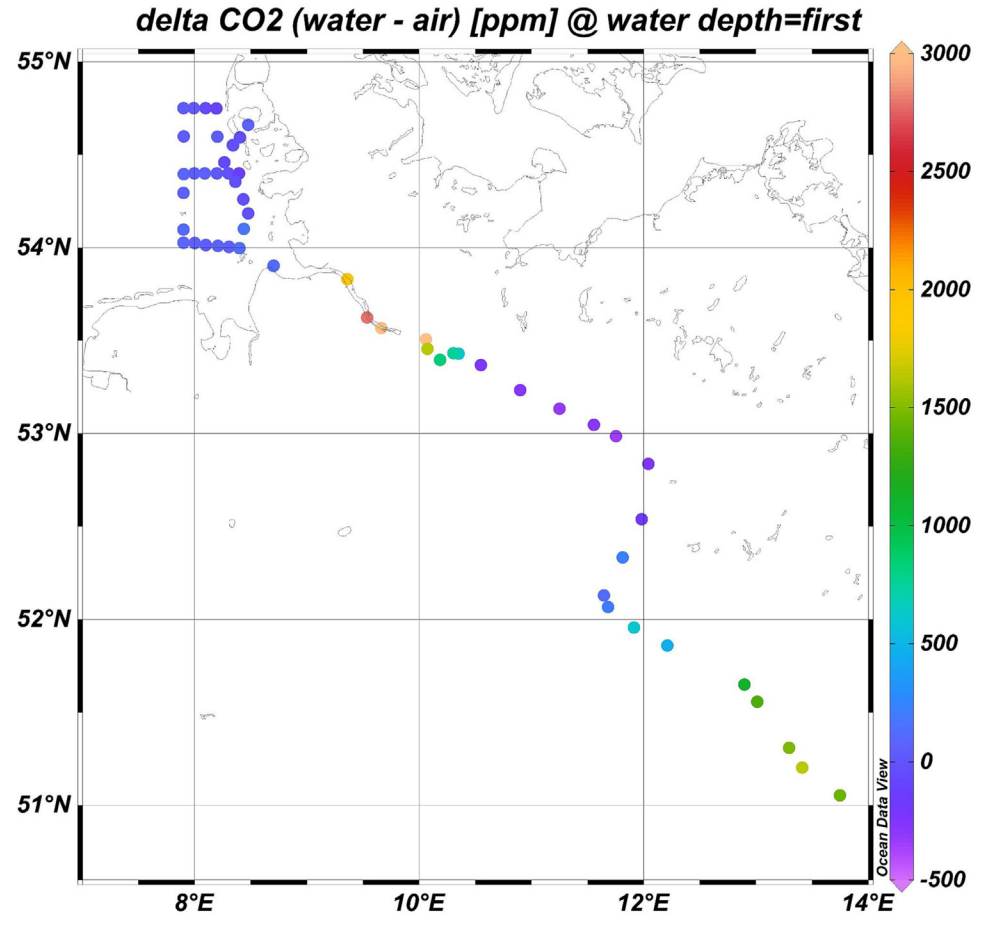


**Fig. 6.** Spatial distribution of deltaCO2 (water-air) concentrations in the freshwater River Elbe, Elbe estuary, and German Bight.

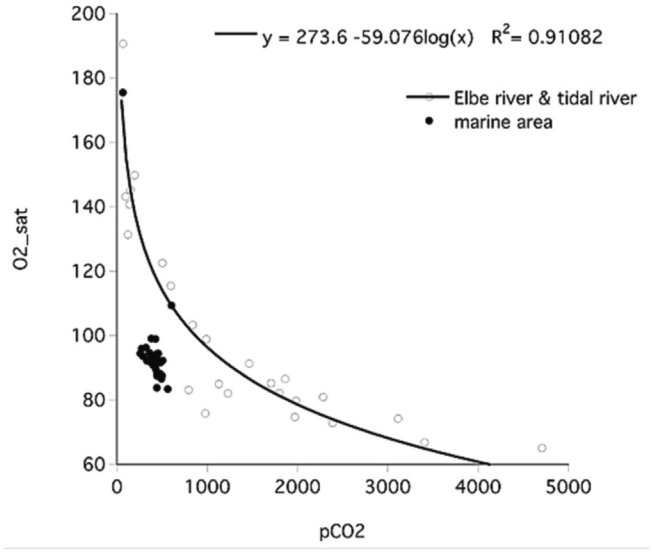


**Fig. 7.** Relationship between pCO2 and O2.

The partial pressure of $CO_2$ ranged between 1128 up to 4709 μatm in the tidal Elbe. Such high values have also been reported for other European rivers such as the Scheldt (5700 μatm; Frankignoulle et al., 1996). Respiration decreased the pH value, which was supported by the correlation between pH and $O_2$-saturation, which both increase due to intensive photosynthesis or decrease due to respiration. The tidal portion of the transect is a hotspot of remineralisation, respiration and nitrification (Norbisrath et al., 2022; Sanders et al., 2018), making the estuary a source of $CO_2$.

### 4.3. Effect of river plume on the marine system

In the marine area, elevated chlorophyll concentrations were mainly found near the west coast of Schleswig-Holstein, probably influenced by the Eider River outflow or the adjacent tidal flats. While most of the measured parameters showed an expected behaviour relative to their individual compartments, the transfer of quantities between the compartments revealed rather complex and sometimes difficult to understand behaviours and patterns, especially when considering a functional quantitative analysis. Nitrogen and phosphorus levels potentially limited phytoplankton growth upstream in the river, but after their release, they were transported out of the estuary into coastal waters where they potentially contributed to coastal eutrophication and fueled algal blooms (Saeck et al., 2013; Wang and Zhang, 2020). Several studies showed that P limitation of primary production in rivers was continued in coastal waters due to the effect of nitrogen-rich river plumes, e.g. in the Mississippi River plume in the Gulf of Mexico (Sylvan et al., 2007), the South China Sea (Xu et al., 2008), but also the North Sea (Burson et al., 2016) whereas the classical view of marine N limitation (Howarth and Marino, 2006) was detected in greater distance in the open sea.

## 5. Conclusions

The first results of this trans-compartment campaign showed that a quantitative understanding of the fate and dynamics of water constituents across compartments, from the spring to the sea, needs enhanced scientific collaboration and awareness. This insight is required in order to finally come to a better integrated understanding of physical, biogeochemical and biological processes from the local to the global scale. The Elbe River was autotrophic in the shallow middle portion in summer, comparable to the illuminated and well mixed epilimnion of a lake. In contrast, the deeper tidal river was heterotrophic upstream of the salinity gradient at low discharge, comparable to the dark and stagnant hypolimnion of a lake. Our approach reveals that the investigation of upstream processes is important in

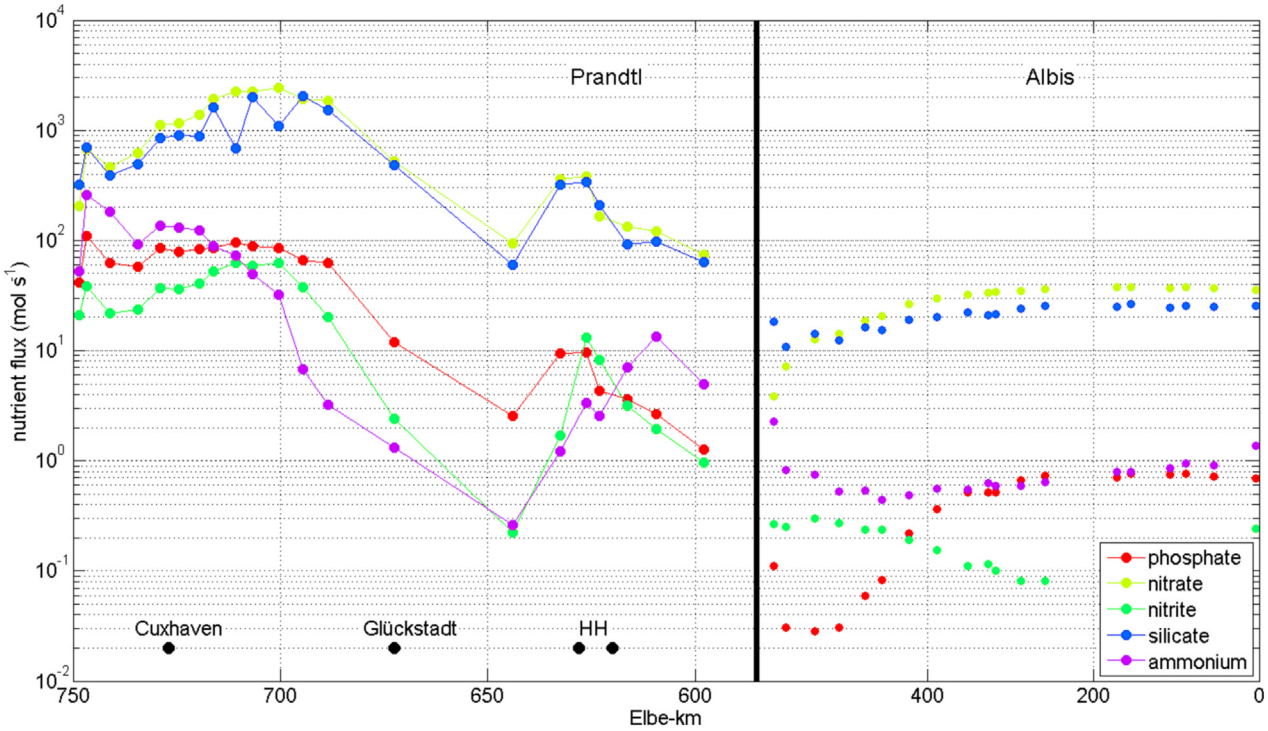


**Fig. 8.** Nutrient fluxes along the river-estuary-coast gradient. The right side is compressed for better visibility of the tidal range. Fluxes have been calculated by multiplying nutrient concentrations by the calculated water fluxes in the river portion and multiplying by 250 $m^3\ s^{-1}$ in the tidal portion. The vertical black line denotes the weir in Geesthacht the separation of the freshwater and the tidally influenced portions of the river.

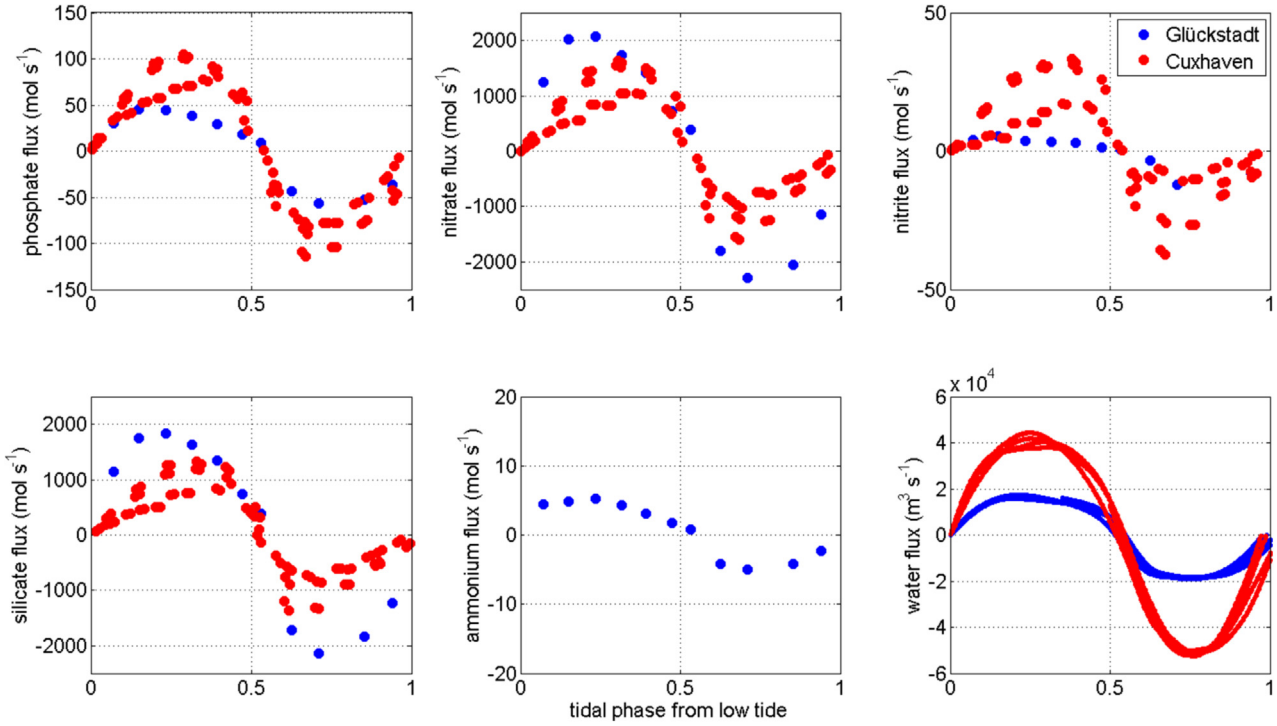


**Fig. 9.** Nutrient fluxes vs. tidal phase in the tidal portion of the River Elbe (Glückstadt, blue dots; FerryBox Cuxhaven: red dots).

understanding downstream system dynamics. Overall, the Lagrangian approach seems to be suitable for investigating the effect of single hydrological extreme events in freshwater on coastal systems in future.

## CRediT authorship contribution statement

**Norbert Kamjunke:** Conceptualization, Investigation, Writing – original draft. **Holger Brix:** Conceptualization, Investigation, Writing – original draft. **Götz Flöser:** Conceptualization, Investigation, Writing – original draft. **Ingeborg Bussmann:** Conceptualization, Investigation, Writing – original draft. **Claudia Schütze:** Conceptualization, Investigation. **Eric P. Achterberg:** Conceptualization, Writing – review & editing. **Uta Ködel:** Investigation. **Philipp Fischer:** Conceptualization, Writing – review & editing. **Louise Rewrie:** Writing – review & editing. **Tina Sanders:** Writing – review & editing. **Dietrich Borchardt:** Conceptualization. **Markus Weitere:** Conceptualization, Writing – review & editing.

## Data availability

Data will be made available on request.

## Declaration of competing interest

The authors declare that they have no known competing financial interests or personal relationships that could have appeared to influence the work reported in this paper.

## Acknowledgements

We thank the captain and crew of RVs *Albis*, *Ludwig Prandtl*, *Littorina* and *Mya II*: S. Bauth, H. Goreczka, U. Link, H. Gerbatsch, and M. Schacht; H. Bornhöft, D. Heinze, M. Gehrung, B. Erbslöh, H. Jebens, D. Kaiser, A. Reese, H. Rust, B. Crénan and F. Geißler; M. Altahan, E. Evers, D. Flindt, H. Krause, F. Witteck, S. Tamm, V. Rzhevsky, and N. Anselm; L. Blum, M. Friedrich, V. Hildebrandt, and H. Schubert. H.-J. Dahlke, S. Willige and F. Zander provided support in the field. A. Hoff, K. Lerche, I. Locker, I. Siebert, M. Tibke and T. Pieplow contributed to the subsequent analyses in the laboratory. C. Viergutz (Federal Institute of Hydrology) provided discharge data for the freshwater River Elbe. This work was supported by funding from the Helmholtz Association within the framework of MOSES (Modular Observation Solutions for Earth Systems).

## Appendix A. Supplementary data

Supplementary data to this article can be found online at https://doi.org/10.1016/j.scitotenv.2023.164421.

## References

Abril, G., Nogueira, M., Etcheber, H., Cabeçadas, G., Lemaire, E., Brogueira, M.J., 2002. Behaviour of organic carbon in nine contrasting European estuaries. Estuar. Coast. Shelf Sci. 54, 241–262.

Amann, T., Weiss, A., Hartmann, J., 2012. Carbon dynamics in the freshwater part of the Elbe estuary, Germany: implications of improving water quality. Estuar. Coast. Shelf Sci. 107, 112–121.

Baschek, B., Schroeder, F., Brix, H., Riethmüller, R., Badewien, T.H., Breitbach, G., et al., 2017. The Coastal Observing System for Northern and Arctic Seas (COSYNA). Ocean Sci. 13, 379–410.

Bazin, P., Jouenne, F., Deton-Cabanillas, A.F., Pérez-Ruzafa, Á., Véron, B., 2014. Complex patterns in phytoplankton and microeukaryote diversity along the estuarine continuum. Hydrobiologia 726, 155–178.

Bessudova, A.Y., Sorokovikova, L.M., Firsova, A.D., Kuz'mina, A.Y., Tomberg, I.V., Likhoshway, Y.V., 2014. Changes in phytoplankton community composition along a salinity gradient from the lower Yenisei River to the Kara Sea, Russia. Bot. Mar. 57, 225–239.

Boehlich, M.J., Strotmann, T., 2008. The Elbe Estuary. Die Küste 74, 288–306.

Bowes, M.J., Gozzard, E., Johnson, A.C., Scarlett, P.M., Roberts, C., Read, D.S., et al., 2012. Spatial and temporal changes in chlorophyll-a concentration in the River Thames basin, UK: are phosphorus concentrations beginning to limit phytoplankton biomass? Sci. Total Environ. 426, 45–55.

Brasse, S., Nellen, M., Seifert, R., Michaelis, W., 2002. The carbon dioxide system in the Elbe estuary. Biogeochemistry 59, 25–40.

Burson, A., Stomp, M., Akil, L., Brussaard, C.P.D., Huisman, J., 2016. Unbalanced reduction of nutrient loads has created an offshore gradient from phosphorus to nitrogen limitation in the North Sea. Limnol. Oceanogr. 61, 869–888.

Bussmann, I., Brix, H., Flöser, G., Ködel, U., Fischer, P., 2021. Detailed patterns of methane distribution in the German bight. Front. Mar. Sci. 8.

Bussmann, I., Koedel, U., Schütze, C., Kamjunke, N., Koschorreck, M., 2022. Spatial variability and hotspots of methane concentrations in a large temperate river. Front. Environ. Sci. 10.

Dähnke, K., Bahlmann, E., Emeis, K., 2008. A nitrate sink in estuaries? An assessment by means of stable nitrate isotopes in the Elbe estuary. Limnol. Oceanogr. 53, 1504–1511.
Dickson, A.G., Sabine, C.L., Christian, J.R., 2007. Guide to Best Practices for Ocean $CO_2$ Measurements. vol. 3. PICES Special Publication.
Dodds, W.K., Cole, J.J., 2007. Expanding the concept of trophic state in aquatic ecosystems: It's not just the autotrophs. Aquat. Sci. 69, 427–439.
Fischer, P., Dietrich, P., Achterberg, E.P., Anselm, N., Brix, H., Bussmann, I., et al., 2021. Effects of measuring devices and sampling strategies on the interpretation of monitoring data for long-term trend analysis. Front. Mar. Sci. 8.
Frankignoulle, M., Bourge, I., Wollast, R., 1996. Atmospheric $CO_2$ fluxes in a highly polluted estuary (the Scheldt). Limnol. Oceanogr. 41, 365–369.
Gattuso, J.P., Frankignoulle, M., Wollast, R., 1998. Carbon and carbonate metabolism in coastal aquatic systems. Annu. Rev. Ecol. Syst. 29, 405–434.
Hardenbicker, P., Weitere, M., Ritz, S., Schöll, F., Fischer, H., 2016. Longitudinal plankton dynamics in the Rivers Rhine and Elbe. River Res. Appl. 32, 1264–1278.
Hari, V., Rakovec, O., Markonis, Y., Hanel, M., Kumar, R., 2020. Increased future occurrences of the exceptional 2018-2019 Central Europe drought under global warming. Sci. Rep. 10, 12207.
Howarth, R.W., Marino, R., 2006. Nitrogen as the limiting nutrient for eutrophication in coastal marine ecosystems: evolving views over three decades. Limnol. Oceanogr. 51, 364–376.
Kamjunke, N., Büttner, O., Jäger, C.G., Marcus, H., von Tümpling, W., Halbedel, S., et al., 2013. Biogeochemical patterns in a river network along a land use gradient. Environ. Monit. Assess. 185, 9221–9236.
Kamjunke, N., Rode, M., Baborowski, M., Kunz, J.V., Zehner, J., Borchardt, D., et al., 2021. High irradiation and low discharge promote the dominant role of phytoplankton in riverine nutrient dynamics. Limnol. Oceanogr. 66, 2648–2660.
Kamjunke, N., Beckers, L.-M., Herzsprung, P., von Tümpling, W., Lechtenfeld, O., Tittel, J., et al., 2022. Lagrangian profiles of riverine autotrophy, organic matter transformation, and micropollutants at extreme drought. Sci. Total Environ. 828, 154243.
Kerner, M., 2000. Interactions between local oxygen deficiencies and heterotrophic microbial processes in the elbe estuary. Limnologica 30, 137–143.
King, S.A., Heffernan, J.B., Cohen, M.J., 2013. Nutrient flux, uptake, and autotrophic limitation in streams and Rivers. Freshw. Sci. 33 (85–98), 14.
Maher, D.T., Eyre, B.D., 2012. Carbon budgets for three autotrophic Australian estuaries: implications for global estimates of the coastal air-water $CO_2$ flux. Glob. Biogeochem. Cycles 26.
Norbisrath, M., Pätsch, J., Dähnke, K., Sanders, T., Schulz, G., van Beusekom, J.E.E., et al., 2022. Metabolic alkalinity release from large port facilities (Hamburg, Germany) and impact on coastal carbon storage. Biogeosciences 19, 5151–5165.
Olli, K., Tamminen, T., Ptacnik, R., 2023. Predictable shifts in diversity and ecosystem function in phytoplankton communities along coastal salinity continua. Limnol.Oceanogr. Lett. 8, 173–180.
Oppermann, R., Schuhmacher, F., Kirchesch, V., 2015. HYDRAX: Ein hydrodynamisches 1-D Modell. Mathematisches Modell und Datenschnittstellen. Bundesanstalt für Gewässerkunde, Koblenz, p. 54.
Petersen, W., 2014. FerryBox systems: state-of-the-art in Europe and future development. J. Mar. Syst. 140, 4–12.
Raymond, P.A., Saiers, J.E., Sobczak, W.V., 2016. Hydrological and biogeochemical controls on watershed dissolved organic matter transport: pulse-shunt concept. Ecology 97, 5–16.
Retamal, L., Bonilla, S., Vincent, W.F., 2008. Optical gradients and phytoplankton production in the Mackenzie River and the coastal Beaufort Sea. Polar Biol. 31, 363–379.
Ritz, S., Fischer, H., 2019. A mass balance of nitrogen in a large lowland river (Elbe, Germany). Water 11, 2383.
Rode, M., Suhr, U., Wriedt, G., 2007. Multi-objective calibration of a river water quality model - information content of calibration data. Ecol. Model. 204, 129–142.
Ruiz Albizuri, J.R., 2018. Effects of Global Warming on Phytoplankton and its Biocontrol in Large Rivers: Insights From a Model Analysis. PhD thesisUniv. Osnabrück, p. 153.
Saeck, E.A., Hadwen, W.L., Rissik, D., O'Brien, K.R., Burford, M.A., 2013. Flow events drive patterns of phytoplankton distribution along a river-estuary-bay continuum. Mar. Freshw. Res. 64, 655–670.
Sanders, T., Schöl, A., Dähnke, K., 2018. Hot spots of nitrification in the Elbe estuary and their impact on nitrate regeneration. Estuar. Coasts 41, 128–138.
Schöl, A., Hein, B., Wyrwa, J., Kirchesch, V., 2014. Modelling water quality in the Elbe and its estuary -large scale and long term applications with focus on the oxygen budget of the estuary. Die Küste 203–232.
Stanev, E.V., Jacob, B., Pein, J., 2019. German bight estuaries: an inter-comparison on the basis of numerical modeling. Cont. Shelf Res. 174, 48–65.
Stokowski, M., Schneider, B., Rehder, G., Kuliński, K., 2020. The characteristics of the CO2 system of the Oder River estuary (Baltic Sea). J. Mar. Syst. 211.
Sukhanova, I.N., Flint, M.V., Mosharov, S.A., Sergeeva, V.M., 2010. Structure of the phytoplankton communities and primary production in the Ob River estuary and over the adjacent Kara Sea shelf. Oceanology 50, 743–758.
Sylvan, J.B., Quigg, A., Tozzi, S., Ammerman, J.W., 2007. Eutrophication-induced phosphorus limitation in the Mississippi River plume: evidence from fast repetition rate fluorometry. Limnol. Oceanogr. 52, 2679–2685.
Turner, R.E., Milan, C.S., Swenson, E.M., Lee, J.M., 2022. Peak chlorophyll a concentrations in the lower Mississippi River from 1997 to 2018. Limnol. Oceanogr. 67, 703–712.
Voynova, Y.G., Brix, H., Petersen, W., Weigelt-Krenz, S., Scharfe, M., 2017. Extreme flood impact on estuarine and coastal biogeochemistry: the 2013 Elbe flood. Biogeosciences 14, 541–557.
Voynova, Y.G., Petersen, W., Gehrung, M., Aßmann, S., King, A.L., 2019. Intertidal regions changing coastal alkalinity: the Wadden Sea-North Sea tidally coupled bioreactor. Limnol. Oceanogr. 64, 1135–1149.
Wang, J., Zhang, Z., 2020. Phytoplankton, dissolved oxygen and nutrient patterns along a eutrophic river-estuary continuum: observation and modeling. J. Environ. Manag. 261.
Weber, U., Attinger, S., Baschek, B., Boike, J., Borchardt, D., Brix, H., et al., 2022. MOSES: a novel observation system to monitor dynamic events across earth compartments. Bull. Am. Meteorol. Soc. 103, E339–E348.
Xu, J., Yin, K., He, L., Yuan, X., Ho, A.Y.T., Harrison, P.J., 2008. Phosphorus limitation in the northern South China Sea during late summer: influence of the Pearl River. Deep-Sea Res. I Oceanogr. Res. Pap. 55, 1330–1342.
Zapata, M., Rodriguez, F., Garrido, J.L., 2000. Separation of chlorophylls and carotenoids from marine phytoplankton: a new HPLC method using a reversed phase C-8 column and pyridine-containing mobile phases. Mar. Ecol. Prog. Ser. 195, 29–45.
Zhang, Y.J., Stanev, E.V., Grashorn, S., 2016. Unstructured-grid model for the North Sea and Baltic Sea: validation against observations. Ocean Model 97, 91–108.